Physics of Plasmas

Density jump as a function of magnetic field for collisionless shocks in pair plasmas: The perpendicular case

Cite as: Phys. Plasmas **26**, 062108 (2019); https://doi.org/10.1063/1.5099000
Submitted: 05 April 2019 . Accepted: 17 May 2019 . Published Online: 07 June 2019

A. Bret, and R. Narayan

Physics of Plasmas ARTICLE scitation.org/journal/php

Density jump as a function of magnetic field for collisionless shocks in pair plasmas: The perpendicular case

Cite as: Phys. Plasmas **26**, 062108 (2019); doi: 10.1063/1.5099000
Submitted: 5 April 2019 · Accepted: 17 May 2019 ·
Published Online: 7 June 2019

A. Bret[1,2] and R. Narayan[3]

AFFILIATIONS

[1]ETSI Industriales, Universidad de Castilla-La Mancha, 13071 Ciudad Real, Spain
[2]Instituto de Investigaciones Energéticas y Aplicaciones Industriales, Campus Universitario de Ciudad Real, 13071 Ciudad Real, Spain
[3]Harvard-Smithsonian Center for Astrophysics, Harvard University, 60 Garden St., Cambridge, Massachusetts 02138, USA

ABSTRACT

In the absence of frequent binary collisions to isotropize the plasma, the fulfillment of the magnetohydrodynamic (MHD) Rankine–Hugoniot jump conditions by collisionless shocks is not trivial. In particular, the presence of an external magnetic field can allow for stable anisotropies, implying some departures from the isotropic MHD jumps. The functional dependence of such anisotropies in terms of the field is yet to be determined. By hypothesizing a kinetic history of the plasma through the shock front, we recently devised a theory of the downstream anisotropy, hence of the density jump, in terms of the field strength for a parallel shock [A. Bret and R. Narayan, J. Plasma Phys. **84**, 905840604 (2018)]. Here, we extend the analysis to the case of a perpendicular shock. We still find that the field reduces the density jump, but the effect is less pronounced than in the parallel case.

I. INTRODUCTION

In a fluid shock, dissipation at the shock front is provided by binary collisions. As a result, the shock front is a few mean-free-path thick.[1] Yet, in a plasma, shockwaves can propagate with a front far smaller than the mean-free-path. For example, the front of the earth bow shock is about 100 km thick, whereas the proton mean-free-path at the same location is of the order of the Sun–Earth distance.[2,3] Here, dissipation is provided by collective plasma effects.[4] Because spatial distances involved in the physics of such shockwaves are smaller than the mean-free-path, these shocks have been called "collisionless shocks".

Since the mechanism sustaining these shocks is different from fluid shocks, one could ask to which extent they fulfill the Rankine–Hugoniot (RH) relations for fluid or magnetohydrodynamic (MHD) shocks. These relations eventually rely on two assumptions: (1) All the matter upstream goes downstream and (2) binary collisions isotropize the distribution function on short time scales. If both assumptions are fulfilled, conservation equations can be written between the upstream and the downstream, and an isotropic equation of state can be used, ensuing RH. In the case of collisionless shocks, (1) is no longer obvious as some upstream particles may get reflected at the front, while others may travel from the downstream to the upstream. Studies conducted so far in this respect found a few percent deviation from RH for the density jump[5] and up to a few tens percent for the downstream temperature.[6]

Regarding assumption (2), namely, that the distribution function is isotropized on short time scales, it has been known for long that the presence of an external magnetic field can jeopardize it.[7] Particle-In-Cell (PIC) simulations recently conducted[8] found a significant reduction of the density jump for the case of a flow-aligned magnetic field, as the field tends to guide the particles downstream,[9] preventing them from isotropizing. Indeed, in the presence of an external field, the Vlasov equation does not impose an isotropic distribution function. It simply limits the range of stable anisotropies instead, through the mirror or the firehose instabilities, for example, Ref. 10. Notably, the kinetic theory sustaining these results has been beautifully verified in the solar wind.[11,12]

Several authors already studied how an anisotropic pressure in the downstream affects the RH jump conditions.[13–16] However, the downstream anisotropy is considered a free parameter in these studies. Our objective is precisely to compute it in terms of the field strength.

In order to devise a theory of the density jump in terms of the field, we recently implemented a model for the case of a magnetic field parallel to the flow.[17] We considered a pair plasma, for simplicity in

such an exploratory work. Electron/ion plasma could add a layer of complexity to the problem, be it because both species might be heated differently at the front.[18–20] The firehose and the mirror instabilities in pair plasmas have been found similar to the ones in electron/ion plasmas,[21] allowing us to use the same stability criteria.

Since the Vlasov equation alone does not impose a unique value of the downstream anisotropy, we made some hypothesis on the thermal history of the plasma through the front. In our previous work on parallel shocks, we assumed the following:[17]

- The upstream is isotropic.
- As it passes through the front, the plasma conserves its temperature perpendicular to the motion. This assumption stems from the double adiabatic theory of Chew–Goldberger-law.[7] The additional entropy generated at the front goes into the direction parallel to the motion since this is the direction of the compression. We labeled "Stage 1" this first stage of the plasma history.
- If Stage 1 is stable, then this is the final state of the downstream.
- If Stage 1 is unstable, then the plasma migrates to the stability threshold (firehose). This is "Stage 2," which is therefore reached only if Stage 1 is unstable.
- In each case, the conservation equations entirely determine the downstream parameters, density jump included.

The goal of this work is to extend the analysis to the perpendicular case. The model was nonrelativistic. We found that for an adiabatic index $\gamma = 5/3$, the density jump in the strong field limit reaches 2, whereas the corresponding MHD value is 4. Notably, for a flow-aligned field, the fluid disconnects from the field in MHD so that the shock properties are independent of the field.[22] Any change in the system when varying the field can therefore be related to a deviation from the MHD behavior.

The system considered in the present work is shown in Fig. 1. The plasma comes from the right and goes leftward. Upstream quantities all bear the subscript "1," and downstream quantities the subscript "2". In order to avoid confusion, we shall not qualify pressures or temperatures with the adjectives "parallel" or "perpendicular" but will refer to the axes x, y, and z instead.

Stage 1 is still defined by a downstream plasma having the same perpendicular (to the motion) temperature as the upstream, that is, $T_{2y} = T_1$. We still assume that the excess entropy generated at the front crossing goes into the x, z directions. Notably, the Vlasov equation imposes a gyrotropic distribution around the field so that $T_{2x} = T_{2z}$ (see, for example, Ref. 23, Sec. 53). As will be shown in the sequel, Stage 1 can be mirror unstable. In case it is, the downstream plasma therefore migrates toward the mirror instability threshold, that is, Stage 2. Whether we deal with Stage 1 or Stage 2, the conservation equations fully determine the state of the downstream, hence the density jump.

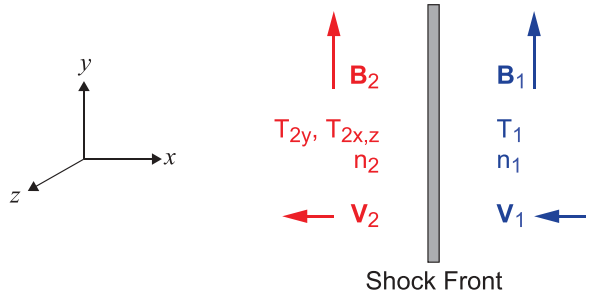

FIG. 1. System considered. The upstream is isotropic. The downstream is anisotropic with $T_{2y} \neq T_{2x,z}$. Due to the orientation of the field, the Vlasov equation imposes $T_{2x} = T_{2z}$.

This article is structured as follows. We start reminding the results of the isotropic MHD theory in Sec. II. The properties and mirror stability of Stage 1 are assessed in Sec. III. Section IV then characterizes the state of the downstream in case it has to move to Stage 2, on the mirror instability threshold. A global picture of the density jump in terms of the field is finally presented in Sec. V, before we reach our conclusions.

II. FORMALISM AND MHD RESULTS

In contrast to the parallel case, the field is not conserved across the shock in MHD and enters the nonrelativistic conservation equations[24]

$$n_1 V_1 = n_2 V_2, \tag{1}$$

$$n_1 V_1^2 + P_1 + \frac{B_1^2}{8\pi} = n_2 V_2^2 + P_{2x} + \frac{B_2^2}{8\pi}, \tag{2}$$

$$V_1 B_1 = V_2 B_2, \tag{3}$$

$$\frac{V_1^2}{2} + \frac{P_1}{n_1} + U_1 + \frac{B_1^2}{4\pi n_1} = \frac{V_2^2}{2} + U_2 + \frac{P_{2x}}{n_2} + \frac{B_2^2}{4\pi n_2}, \tag{4}$$

where U is the internal energy of the fluid. As in the parallel case, the downstream pressure entering the equations is the one along the x axis, which is the direction of the fluid motion (see Ref. 25, Sec. 40-3). Here, the direction of motion and the field are perpendicular.

We now introduce the dimensionless parameters

$$r = \frac{n_2}{n_1}, \quad A_2 = \frac{T_{2x,z}}{T_{2y}}, \quad \chi_1^2 = \frac{V_1^2}{P_1/n_1}, \quad M_{A1}^2 = \frac{n_1 V_1^2}{B_1^2/4\pi}, \tag{5}$$

where the downstream anisotropy reads $A_2 = T_{2x}/T_{2y} = T_{2z}/T_{2y}$. The χ_1 parameter looks like a Mach number, but since we force the degrees of freedom of the plasma, it is preferable to deter such an interpretation to the end of the analysis.

In order to make the junction with PIC simulations (see Ref. 26 and references therein) and with our previous treatment of the parallel case, we also introduce the dimensionless parameter

$$\sigma = \frac{B_1^2/4\pi}{n_1 V_1^2} = \frac{1}{M_{A1}^2}. \tag{6}$$

We now remind the MHD results for a perpendicular shock.

A. MHD results

We here set $U_i = P_i/n_i(\gamma - 1)$. From Eq. (2), one can express P_{2x} in terms of n_2 and the upstream quantities [also using Eqs. (1) and (3)]. We then do the same with Eq. (4) and equate the 2 expressions of P_{2x}. The resulting equation for n_2 is a 3rd degree polynomial in r. It can be factored by $(r - 1)$ since the conservation equations obviously admit plasma continuity as a solution. The remaining 2nd order polynomial has one negative root. The positive one is[27]

$$r = \frac{\gamma M_1^2 + M_{A1}^2\left(2 + (\gamma - 1)M_1^2\right) - \sqrt{\Delta}}{2(\gamma - 2)M_1^2}, \quad \text{with}$$

$$\Delta = 4(\gamma - \gamma^2 + 2)M_1^4 M_{A1}^2 + \left[\gamma M_1^2 + M_{A1}^1\left(2 + (\gamma - 1)M_1^2\right)\right]^2, \tag{7}$$

where we defined the upstream Mach number $M_1^2 = n_1 V_1^2/\gamma P_1 \equiv V_1^2/C_{s1}^2$ (C_{s1} is the upstream speed of sound).

The density jump is larger than unity for

$$M_1^2 > \frac{M_{A1}^2}{\sqrt{M_{A1}^2 - 1}} \Rightarrow V_1^2 > C_{s1}^2 + V_{A1}^2 \tag{8}$$

with $V_{A1}^2 = V_1^2/B_1^2/4\pi n_1$. Figure 2-left plots Eq. (7) over the domain defined by Eq. (8).

In terms of the parameters χ_1, σ defined by Eqs. (5) and (6), we find

$$r < 1 \text{ for } \sigma > \frac{\chi_1^2 - \gamma}{\chi_1^2} \tag{9}$$

so that the shock solutions are limited by the strength of the field. In other words, too strong a field switches off the MHD shock. Figure 2-right pictures the portion of the (χ_1, σ) phase space, yielding shock solutions for $\gamma = 5/3$. The requirement $r > 1$ imposes $\chi_1^2 > \gamma$, that is, $M_1 > 1$.

III. STAGE 1: DOWNSTREAM WITH $T_{2y} = T_{1y} = T_1$

Since the upstream is considered isotropic, we simply set $U_1 = P_1/n_1(\gamma - 1)$ in Eq. (4). In addition, we consider $\gamma = 5/3$ in the sequel.

As specified earlier, our ansatz is that T_y is conserved when crossing the front, while the entropy increase goes in the $T_{x,z}$ directions. In order to express U_2 accounting for this ansatz, we start from

$$U_2 = \frac{1}{2n_2}(P_{2y} + P_{2x} + P_{2z}) = \frac{1}{2}(k_B T_{2y} + 2k_B T_{2x}). \tag{10}$$

Using $T_{2y} = T_1$, we get

$$U_2 = \frac{1}{2}(k_B T_1 + 2k_B T_{2x}) = \frac{1}{2}\left(\frac{P_1}{n_1} + 2\frac{P_{2x}}{n_2}\right). \tag{11}$$

We now substitute this expression into Eq. (4) and apply the resolution method described for the simple MHD case. We find only 2 solutions for the jump. One is $r = 1$, and the other is

$$r = \frac{3M_{A1}^2\chi_1^2}{M_{A1}^2(\chi_1^2 + 4) + 2\chi_1^2}, = \frac{3\chi_1^2}{(2\sigma + 1)\chi_1^2 + 4}. \tag{12}$$

At low B_1 (high M_{A1}), the corresponding strong shock has $r = 3$, which corresponds to a strong 2D shock. Then, increasing B_1 lowers r. This jump is larger than unity for

$$\chi_1^2 > \frac{2M_{A1}^2}{M_{A1}^2 - 1} \Rightarrow V_1^2 > V_{A1}^2 + 2C_s^2. \tag{13}$$

A notable consequence of Eq. (12) for the density jump is that

$$r < 1 \text{ for } \sigma > \frac{\chi_1^2 - 2}{\chi_1^2} \tag{14}$$

clearly reminiscent of Eq. (9), the corresponding relation for the MHD case. Our ansatz for Stage 1 eventually leaves the downstream plasma with 2 degrees of freedom, hence an effective adiabatic index of 2. Equation (14) is therefore coherent with Eq. (9), and the strong shock limit of Stage 1, namely, $r = 3$, is also coherent with the effective γ.

We now need to compute the Stage 1 anisotropy in order to assess its stability. Some algebra shows that

$$A_2 = \frac{T_{2x,z}}{T_{2y}} = \frac{P_{2x}/n_2}{P_1/n_1} = \frac{1}{r}\frac{P_{2x}}{P_1}, \tag{15}$$

where P_{2x} is computed from Eq. (2). The result is

$$A_2 = \frac{1}{r} - \frac{(r-1)\chi_1^2(r^2 + r - 2M_{A1}^2)}{2M_{A1}^2 r^2}. \tag{16}$$

Clearly, $r = 1$ gives $A_2 = 1$ so that $A_2 = 1$ on the frontier defined by (13). Figure 3 plots the anisotropy A_2 given in Eq. (16) over the domain defined by (13). We have $A_2 > 1$. As a consequence, Stage 1 could be mirror unstable.

A. Mirror stability of Stage 1

The threshold for the mirror instability is defined by[10]

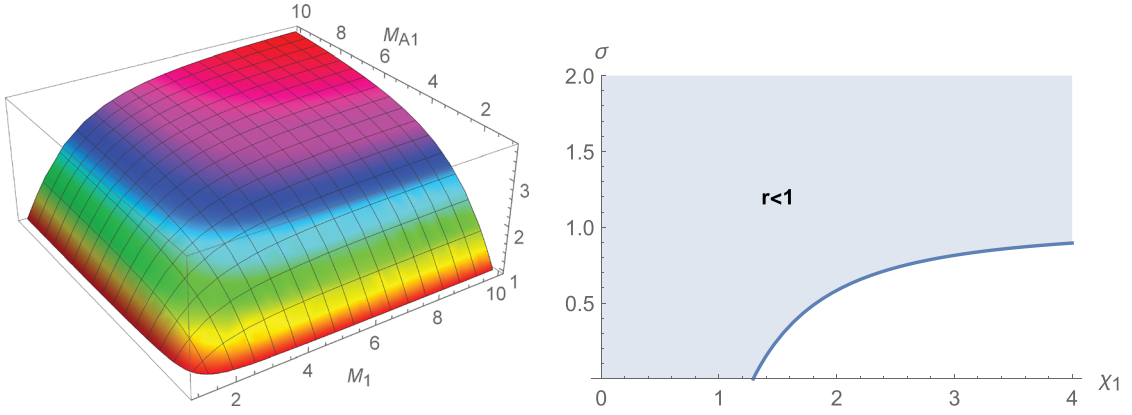

FIG. 2. Left: Plot of the MHD density jump [Eq. (7)] in terms of the upstream Mach number M_1 and Alfvén Mach number M_{A1} for $\gamma = 5/3$ and over the domain defined by (8). Right: Domain of the (χ_1, σ) phase space yielding shock solutions according to Eq. (8) and for $\gamma = 5/3$.

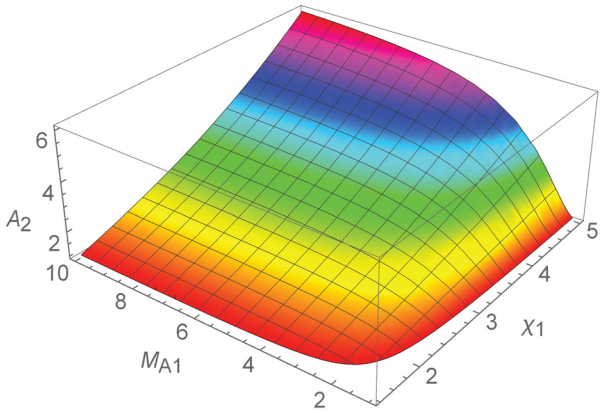

FIG. 3. Plot of the anisotropy A_2 given in Eq. (16) over the range defined by (13). $\gamma = 5/3$.

$$\frac{T_{2\perp}}{T_{2\parallel}} = A_2 = \frac{T_{2xz}}{T_{2y}} = 1 + \frac{1}{\beta_{2\parallel}}, \tag{17}$$

where the subscripts $\parallel$ and $\perp$ refer to parallel and perpendicular to the field. The parameter $\beta_{2\parallel}$ can be expressed from

$$\beta_{2\parallel} = \frac{n_2 T_{2\parallel}}{B_2^2/8\pi} = \frac{n_2 T_{2y}}{B_2^2/8\pi} = \frac{2}{r\sigma\chi_1^2}. \tag{18}$$

Equations (17) and (18) yield a stability condition for Stage 1 defined by the following 3rd degree equation in σ:

$$A_2 = 1 + \frac{r\sigma\chi_1^2}{2} \iff \sum_{k=0}^{3} a_k \sigma^k = 0, \tag{19}$$

where

$$\begin{aligned} a_0 &= 4\left(\chi_1^2 - 2\right)\left(\chi_1^2 + 1\right)\left(\chi_1^2 + 4\right), \\ a_1 &= -3\chi_1^2\left(13\chi_1^4 - 4\chi_1^2 + 16\right), \\ a_2 &= 12\chi_1^4\left(\chi_1^2 - 2\right), \\ a_3 &= -4\chi_1^6. \end{aligned} \tag{20}$$

With *Mathematica*, this equation can be solved exactly. Two roots are imaginary, and only one is real. The threshold $\sigma(\chi_1)$ thus defined is plotted in Fig. 4, and its full expression is reported in the Appendix, Eq. (A1). In the strong shock limit $\chi_1 = \infty$, the stability frontier reaches the asymptotic value σ_a

$$\sigma_a = 1 - \frac{3}{2}\sqrt[3]{\sqrt{2}+1} + \frac{3}{2\sqrt[3]{\sqrt{2}+1}} \sim 0.106. \tag{21}$$

The stability threshold attains $\sigma = 0$ for $\chi_1 = \sqrt{2}$. A Taylor expansion near $\chi_1 = \sqrt{2}$ gives

$$\sigma = \frac{2^{3/2}}{5}\left(\chi_1 - \sqrt{2}\right) + \mathcal{O}(\chi_1 - \sqrt{2})^2. \tag{22}$$

The frontier reaches a maximum for $\chi_1 = 2.42$ and $\sigma_c = 0.14$.

We also picture in Fig. 4 the limit (14) beyond which $r < 1$. Stage 1 has stable solutions only in the shaded region.

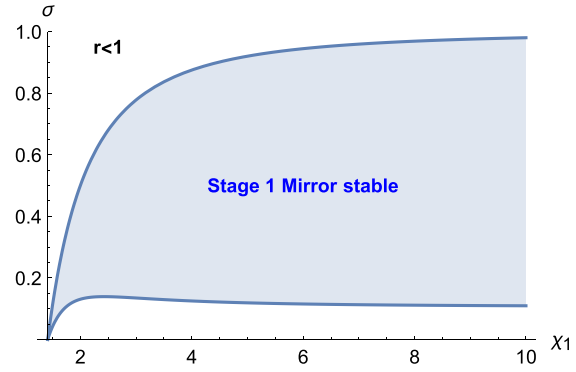

FIG. 4. Domain of the (χ_1, σ) phase space where Stage 1 defines a shock and is stable. Below the lower frontier, defined by Eq. (17), the field is too weak to stabilize the anisotropy. Above the upper frontier, defined by Eq. (14), the field switches off the shock.

We therefore find that Stage 1 ($T_{2y} = T_1$) always has $A_2 > 1$ and can be stabilized with a magnetic field, as shown by the shaded region in Fig. 4. If it is mirror unstable, then the downstream plasma will migrate toward the mirror stability threshold. We shall now see that in this case, the conservation equations determine uniquely all the downstream properties.

IV. STAGE 2

In case Stage 1 is unstable, it has $A_2 > 1$ (see Fig. 3), and so the downstream plasma moves toward the mirror threshold. We therefore impose now

$$A_2 = 1 + \frac{1}{\beta_{2\parallel}}. \tag{23}$$

In order to compute the density jump, we start again from

$$U_2 = \frac{1}{2}(k_B T_{2y} + 2k_B T_{2x}).$$

Being in the mirror threshold, Eq. (23) imposes $T_{2y} = T_{2x} - B_2^2/8\pi n_2$, so that

$$U_2 = \frac{1}{2}\left(k_B T_{2x} - \frac{B_2^2/8\pi}{n_2} + 2k_B T_{2x}\right) = \frac{1}{2n_2}\left(3P_{2x} - \frac{B_2^2}{8\pi}\right). \tag{24}$$

We then apply the same method as before, replacing U_2 in Eq. (4) by the above expression. We find the following 3rd degree polynomial equation for the density jump r

$$\begin{aligned} P(r) = 2\chi_1^2 r^3 &+ \left(\frac{10}{\sigma} + \frac{2\chi_1^2}{\sigma} - 4\chi_1^2\right) r^2 \\ &- \left(\frac{10}{\sigma} + \frac{10\chi_1^2}{\sigma} + 5\chi_1^2\right) r + \frac{8\chi_1^2}{\sigma} = 0. \end{aligned} \tag{25}$$

We now determine upon which conditions on (σ, χ_1), this equation offers real solutions for the density jump r.

As an even degree polynomial, it has always at least one real root. Indeed, we shall see that there are either 1 or 3 real roots. In case there are 3 roots, 2 of them are >0 and one is <0. Figure 5 plots the 2 positive roots in terms of (χ_1, σ). They join on a frontier studied below,

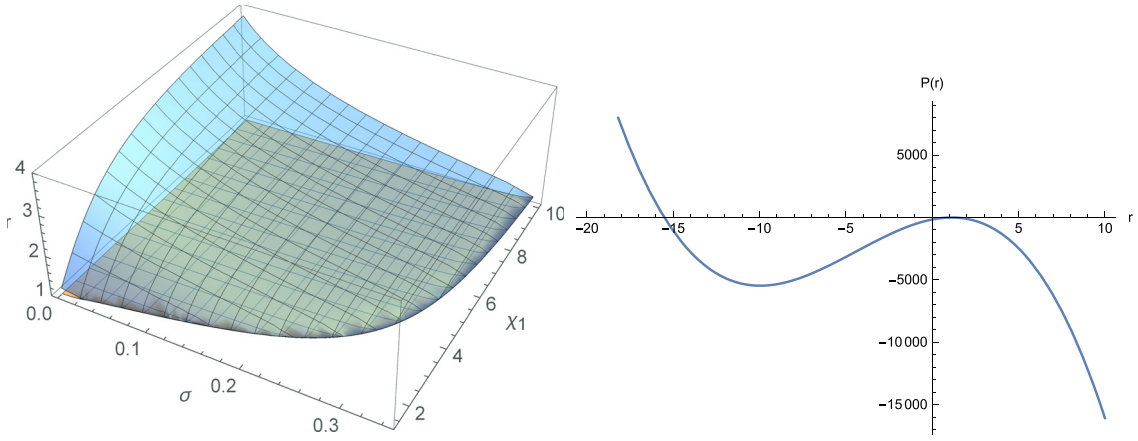

FIG. 5. Left: Plot of the 2 real roots of Eq. (25). The physical one is the upper one, which merges with the MHD solution for $\sigma = 0$. Right: Typical shape of $P(r)$, here with $\sigma = 0.2$ and $\chi_1 = 2$.

and the physical one is the upper one as it merges with the MHD solution for $\sigma = 0$.

In order to make sense of the result, it is useful to further study the polynomial (25). Let us symbolically write it as

$$P(r) = ar^3 + br^2 + cr + d$$

and denote its 3 roots r_1, r_2, and r_3. They fulfill the identities

$$\prod_i r_i = -d/a = -4/\sigma < 0, \tag{26}$$

$$\sum_i r_i = -b/a = -2 - \frac{1}{\sigma}\left(1 + \frac{5}{\chi_1^2}\right) < 0. \tag{27}$$

In addition, one can compute $\partial P/\partial r$ and show that it always has 2 purely real roots. Because $a < 0$, the shape of $P(r)$ is typically like the one pictured in Fig. 5-right. As long as we have 3 real roots, 2 of them are positive and the third has to be negative to fulfill (26). When the value of the right extremum falls below 0, the 2 corresponding real roots become imaginary conjugate and the third one remains negative.

Stage 2 therefore offers solutions as long as this right extremum on Fig. 5-right is larger than 0. Since $\partial P/\partial r$ is of 2nd order, it can be solved exactly, giving the values of $r_\pm$ so that $\partial P/\partial r(r_\pm) = 0$. The largest extremum of $P(r)$ is found at

$$r_+ = \frac{(4\sigma + 2)\chi_1^2 + 10 + \sqrt{\Delta}}{6\sigma\chi_1^2}, \text{ with}$$
$$\Delta = (46\sigma^2 + 76\sigma + 4)\chi_1^4 + 20(7\sigma + 2)\chi_1^2 + 100. \tag{28}$$

The equation $P(r_+) = 0$ then gives the region of the (χ_1, σ) phase space where Stage 2 offers solutions. This region is plotted in Fig. 6 together with the stability region of Stage 1. There is a significant overlap between the two domains. Namely, there is a (χ_1, σ) domain where Stage 1 is stable, while Stage 2 already offers solutions. In such a case and according to the kinetic history, we hypothesized that the downstream should settle in Stage 1 since it first goes through this stage.

V. PUTTING THE 2 STAGES TOGETHER

We can now put the 2 stages together and plot the jump in terms of σ. This is done in Fig. 7. It is interesting to compare with the result (7) of "isotropic" MHD. The dashed lines in Fig. 7 picture the isotropic MHD result (7).

At low σ, the field is too weak to stabilize Stage 1 so that the system ends in Stage 2. Then, the field becomes strong enough to stabilize Stage 1, even though Stage 2 still offers solutions. In that case, the system settles in Stage 1 since this is the first stage of its kinetic history. As a result, the corresponding part of the jump for Stage 2 is in thin lines in the figure. Then, for even larger fields, Stage 2 no longer has solutions, while Stage 1 is stable. There, the jump is unambiguously given by Stage 1.

As a consequence of the downstream anisotropy allowed by the field, the density jump is smaller than that in isotropic MHD. Yet, unlike the jump reduction in the parallel case which can reach 50%, the difference here is minor for at least two reasons. To start with, the isotropic MHD jump decreases with the field, whereas it is independent of the field in the parallel case. Then, the microphysical explanation highlighted in the parallel case could also play a role. More precisely, the downstream anisotropy in the parallel case is related to the effect of the flow aligned field which guides the particles in the

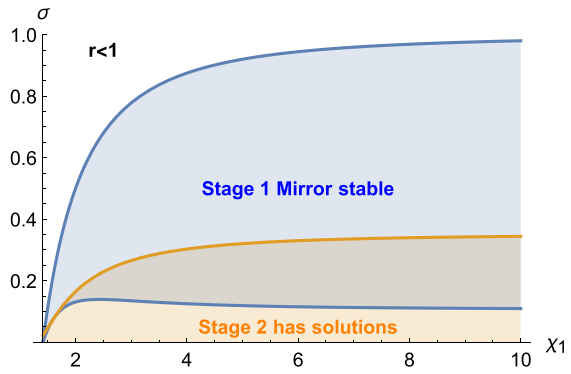

FIG. 6. Stage 1 is stable and defines a shock between the two blue lines. Stage 2 offers solutions below the orange line. The orange curve is always above the lower blue one, even at low χ_1, where they are exactly tangent (at least numerically) to each other for $\chi_1 = 1.6$.

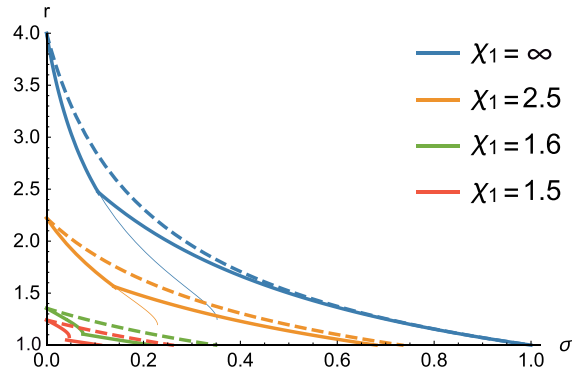

FIG. 7. Density jump in terms of σ. At low σ, Stage 2 offers solutions. At large σ, the jump is given by Stage 1, which is stable. When both stages offer solutions at once, the physical solution is Stage 1. This is the reason why part of the Stage 2 solutions (low σ) are pictured in thin lines. The dashed lines picture the isotropic MHD result (7).

downstream, preventing isotropization.[8,9] In the present perpendicular case, the field rather helps the shock formation instead of hindering it in the parallel case (see the conclusion).

VI. CONCLUSION

We have investigated the departure from MHD of the density jump of a nonrelativistic perpendicular shock. Such a departure comes from a pressure anisotropy in the downstream (the upstream is assumed isotropic). Vlasov theory alone cannot pinpoint any definite downstream anisotropy. It only allows for a range of stable anisotropic plasmas instead. In order to derive a theory of the downstream anisotropy in terms of the field, we made an ansatz on the kinetic history of the plasma as it crosses the shock front.

The departure from MHD is less pronounced than in the parallel case, consistent with what is expected from collisionless shock formation theory. Indeed, when two collisionless plasma shells collide, they overlap and the overlying region becomes unstable to competing streaming instabilities.[28,29] The shock starts forming when the turbulence arising from the growth of instabilities becomes capable of blocking the incoming flow.[30–34] Yet, a parallel magnetic field will tend to guide the particles in the overlapping region, hindering the density build up. In contrast, a perpendicular field will help the particles to remain in the overlapping region, contributing to the density build up.

Our model requires $\chi_1^2 > 2$. Since the upstream Mach number M_1 verifies $M_1^2 = \chi_1^2/\gamma$, choosing $\gamma = 5/3$ imposes $M_1 > \sqrt{2/\frac{5}{3}} = 1.1$. Indeed, the assumed kinetic history yields no shock solution for $1 < M_1 < 1.1$. As evidenced in Eq. (9) and Fig. 2-right, this stands in contrast to the MHD case where solutions are available from $M_1 > 1$. This difference is only notable for weak fields as both models share the same shock existence criteria for $\sigma \sim 1$, i.e., $\chi_1 \gg 1$, as can be seen comparing Eqs. (9) and (14). Our analysis shows that in the weak shock limit, the conservation equations forbid the conservation of the temperature parallel to the field.

Future studies contemplate the extension to the relativistic regime, the exploration of oblique field orientations, or PIC simulations aiming at assessing the assumed kinetic history of the plasma. To our knowledge, no PIC simulations have been performed in the strong field regime, namely, $\sigma \sim 1$. While our scenario should hold in the limit $\sigma = \infty$, PIC simulations will be needed to assess how instabilities in the shock transition, for example, could affect the result for $\sigma \sim 1$ for the present perpendicular case and for $\sigma \gg 1$ in the parallel case.

ACKNOWLEDGMENTS

A.B. acknowledges support of Grant Nos. ENE2016-75703-R from the Spanish Ministerio de Educación and SBPLY/17/180501/000264 from the Junta de Comunidades de Castilla-La Mancha. R.N. acknowledges support from the NSF via Grant No. AST-1816420. A.B. thanks the Black Hole Initiative (BHI) at Harvard University for hospitality, and R.N. thanks the BHI for support. The BHI is funded by a grant from the John Templeton Foundation.

APPENDIX: STABILITY THRESHOLD FOR STAGE 1

Stage 1 discussed in Sec. III is stable for a strong enough field. It turns mirror unstable for σ lower than

$$\sigma(\chi_1) = \frac{\mathcal{A} - \mathcal{B} + 2(\chi_1^2 - 2)}{2\chi_1^2} \tag{A1}$$

with

$$\mathcal{A} = \frac{3^{2/3}\chi_1(3\chi_1^2 + 4)}{\mathcal{C}},$$
$$\mathcal{B} = 3^{1/3}\chi_1\mathcal{C},$$
$$\mathcal{C} = \left[9\chi_1(\chi_1^2 - 2) + \sqrt{6}\sqrt{27\chi_1^6 + 126\chi_1^2 + 32}\right]^{1/3}.$$

REFERENCES

[1] I. A. B. Zel'dovich and Y. P. Raizer, *Physics of Shock Waves and High-Temperature Hydrodynamic Phenomena*, Dover books on physics (Dover Publications, 2002).
[2] S. D. Bale, F. S. Mozer, and T. S. Horbury, "Density-transition scale at quasi-perpendicular collisionless shocks," Phys. Rev. Lett. **91**, 265004 (2003).
[3] S. J. Schwartz, E. Henley, J. Mitchell, and V. Krasnoselskikh, "Electron temperature gradient scale at collisionless shocks," Phys. Rev. Lett. **107**, 215002 (2011).
[4] R. Z. Sagdeev, "Cooperative phenomena and shock waves in collisionless plasmas," Rev. Plasma Phys. **4**, 23 (1966); available at http://adsabs.harvard.edu/abs/1966RvPP....4...23S.
[5] A. Stockem, F. Fiúza, R. A. Fonseca, and L. O. Silva, "The impact of kinetic effects on the properties of relativistic electron-positron shocks," Plasma Phys. Controlled Fusion **54**, 125004 (2012).
[6] D. Caprioli and A. Spitkovsky, "Simulations of ion acceleration at nonrelativistic shocks. i. acceleration efficiency," Astrophys. J. **783**, 91 (2014).
[7] G. F. Chew, M. L. Goldberger, and F. E. Low, "The Boltzmann equation and the one-fluid hydromagnetic equations in the absence of particle collisions," Proc. R. Soc. London, Ser. A **236**(1204), 112–118 (1956).
[8] A. Bret, A. Pe'er, L. Sironi, A. Sa¸dowski, and R. Narayan, "Kinetic inhibition of magnetohydrodynamics shocks in the vicinity of a parallel magnetic field," J. Plasma Phys. **83**, 715830201 (2017).
[9] A. Bret, "Particles trajectories in weibel magnetic filaments with a flow-aligned magnetic field," J. Plasma Phys. **82**, 905820403 (2016).
[10] S. P. Gary, *Theory of Space Plasma Microinstabilities*, Cambridge atmospheric and space science series (Cambridge University Press, 1993).
[11] B. A. Maruca, J. C. Kasper, and S. D. Bale, "What are the relative roles of heating and cooling in generating solar wind temperature anisotropies?," Phys. Rev. Lett. **107**, 201101 (2011).

[12]R. Schlickeiser, M. J. Michno, D. Ibscher, M. Lazar, and T. Skoda, "Modified temperature-anisotropy instability thresholds in the solar wind," Phys. Rev. Lett. **107**, 201102 (2011).
[13]H. Karimabadi, D. Krauss-Varban, and N. Omidi, "Temperature anisotropy effects and the generation of anomalous slow shocks," Geophys. Res. Lett. **22**(20), 2689–2692, https://doi.org/10.1029/95GL02788 (1995).
[14]N. V. Erkaev, D. F. Vogl, and H. K. Biernat, "Solution for jump conditions at fast shocks in an anisotropic magnetized plasma," J. Plasma Phys. **64**, 561–578 (2000).
[15]D. F. Vogl, H. K. Biernat, N. V. Erkaev, C. J. Farrugia, and S. Mühlbachler, "Jump conditions for pressure anisotropy and comparison with the earth's bow shock," Nonlinear Processes Geophys. **8**(3), 167–174 (2001).
[16]D. Gerbig and R. Schlickeiser, "Jump conditions for relativistic magnetohydrodynamic shocks in a gyrotropic plasma," Astrophys. J. **733**(1), 32 (2011).
[17]A. Bret and R. Narayan, "Density jump as a function of magnetic field strength for parallel collisionless shocks in pair plasmas," J. Plasma Phys. **84**, 905840604 (2018).
[18]X. Guo, L. Sironi, and R. Narayan, "Electron heating in low-Mach-number perpendicular shocks. I. Heating mechanism," Astrophys. J. **851**, 134 (2017).
[19]X. Guo, L. Sironi, and R. Narayan, "Electron heating in low Mach number perpendicular shocks. II. Dependence on the pre-shock conditions," Astrophys. J. **858**, 95 (2018).
[20]M. Miceli, S. Orlando, D. N. Burrows, K. A. Frank, C. Argiroffi, F. Reale, G. Peres, O. Petruk, and F. Bocchino, "Collisionless shock heating of heavy ions in SN 1987A," Nat. Astron. **3**, 236–241 (2019).
[21]S. P. Gary and H. Karimabadi, "Fluctuations in electron-positron plasmas: Linear theory and implications for turbulence," Phys. Plasmas **16**(4), 042104 (2009).
[22]A. Lichnerowicz, "Shock waves in relativistic magnetohydrodynamics under general assumptions," J. Math. Phys. **17**, 2135–2142 (1976).
[23]L. D. Landau and E. M. Lifshitz, *Course of Theoretical Physics, Physical Kinetics* (Elsevier, Oxford, 1981), Vol. 10.
[24]M. K. Russell, *Plasma Physics for Astrophysics* (Princeton University Press, Princeton, NJ, 2005).
[25]R. P. Feynman, R. B. Leighton, and M. L. Sands, *The Feynman Lectures on Physics*, Number v. 2 in The Feynman lectures on physics (Pearson/Addison-Wesley, 1963).
[26]A. Marcowith, A. Bret, A. Bykov, M. E. Dieckman, L. Drury, B. Lembège, M. Lemoine, G. Morlino, G. Murphy, G. Pelletier, I. Plotnikov, B. Reville, M. Riquelme, L. Sironi, and A. S. Novo, "The microphysics of collisionless shock waves," Rep. Prog. Phys. **79**, 046901 (2016).
[27]R. Fitzpatrick, *Plasma Physics: An Introduction* (Taylor and Francis, 2014).
[28]A. Bret, L. Gremillet, D. Bénisti, and E. Lefebvre, "Exact relativistic kinetic theory of an electron-beam-plasma system: Hierarchy of the competing modes in the system-parameter space," Phys. Rev. Lett. **100**, 205008 (2008).
[29]A. Bret, L. Gremillet, and M. E. Dieckmann, "Multidimensional electron beam-plasma instabilities in the relativistic regime," Phys. Plasmas **17**, 120501 (2010).
[30]A. Bret, A. Stockem, F. Fiuza, C. Ruyer, L. Gremillet, R. Narayan, and L. O. Silva, "Collisionless shock formation, spontaneous electromagnetic fluctuations, and streaming instabilities," Phys. Plasmas **20**(4), 042102 (2013).
[31]A. Bret, A. Stockem, R. Narayan, and L. O. Silva, "Collisionless weibel shocks: Full formation mechanism and timing," Phys. Plasmas **21**(7), 072301 (2014).
[32]C. Ruyer, L. Gremillet, A. Debayle, and G. Bonnaud, "Nonlinear dynamics of the ion weibel-filamentation instability: An analytical model for the evolution of the plasma and spectral properties," Phys. Plasmas **22**(3), 032102 (2015).
[33]A. Stockem Novo, A. Bret, R. A. Fonseca, and L. O. Silva, "Shock formation in electron-ion plasmas: Mechanism and timing," Astrophys. J. Lett. **803**, L29 (2015).
[34]C. Ruyer, L. Gremillet, G. Bonnaud, and C. Riconda, "Analytical predictions of field and plasma dynamics during nonlinear weibel-mediated flow collisions," Phys. Rev. Lett. **117**, 065001 (2016).